LAWRENCE
LIVERMORE
NATIONAL
LABORATORY

LLNL-CONF-570163

Atomic data of tungsten for current and future uses in fusion and plasma science

J. Clementson, P. Beiersdorfer, T. Lennartsson

August 6, 2012

22nd International Conference on the Application of Accelerators in Research and Industry
Fort Worth, TX, United States
August 5, 2012 through August 10, 2012

Disclaimer

Atomic Data of Tungsten for Current and Future Uses in Fusion and Plasma Science

J. Clementson[a], P. Beiersdorfer[a], and T. Lennartsson[b, 1]

[a]*Physics Division, Lawrence Livermore National Laboratory, Livermore, California 94550, USA*

[b]*Lund Observatory, Lund University, SE-221 00 Lund, Sweden*

Abstract. Atomic physics has played an important role throughout the history of experimental plasma physics. For example, accurate knowledge of atomic properties has been crucial for understanding the plasma energy balance and for diagnostic development. With the shift in magnetic fusion research toward high-temperature burning plasmas like those expected to be found in the ITER tokamak, the atomic physics of tungsten has become of importance. Tungsten will be a constituent of ITER plasmas because of its use as a plasma-facing material able to withstand high heat loads with lower tritium retention than other possible materials. Already, ITER diagnostics are being developed based on using tungsten radiation. In particular, the ITER Core Imaging X-ray Spectrometer (CIXS), which is designed to measure the core ion temperature and bulk plasma motion, is being based on the x-ray emission of neonlike tungsten ions (W^{64+}). In addition, tungsten emission will at ITER be measured by extreme ultraviolet (EUV) and optical spectrometers to determine its concentration in the plasma and to assess power loss and tungsten sputtering rates. On present-day tokamaks tungsten measurements are therefore being performed in preparation of ITER. Tungsten has very complex spectra and most are still unknown. The WOLFRAM project at Livermore aims to produce data for tungsten in various spectra bands: L-shell x-ray emission for CIXS development, soft x-ray and EUV M- and N-shell tungsten emission for understanding the edge radiation from ITER plasmas and contemporary tokamaks, and O-shell emission for developing spectral diagnostics of the ITER divertor.

Keywords: spectroscopic plasma diagnostics, atomic data, tungsten, tokamak, ITER, EBIT

PACS: 32.30.Jc, 32.30.Rj, 32.70.Fw, 32.70.Jz, 52.25.Vy, 52.70.Kz, 52.70.La

[1] Present address:

INTRODUCTION

Accurate atomic data on tungsten ions ($Z = 74$) have gained importance in the last few years as tungsten research has become frequent at magnetic fusion facilities. The interest in tungsten spectra is spurred by the design choice of the heavy element as a plasma-facing material in the ITER divertor [1] due to its favorable physical and chemical properties: it has a high melting point, low sputtering yields, high-energy sputtering threshold, and low tritium retention. On the agenda for several present-day fusion machines is to operate with tungsten components to learn machine behavior and study the effects of tungsten-seeded plasmas. Especially the JET tokamak is pursuing this with the recent installation of the ITER-like wall [2] and the ASDEX Upgrade tokamak that for many years has been the leading experiment for tungsten tokamak studies [3]. Tungsten injection experiments at several other magnetic fusion facilities have focused on the spectral signatures or particle transport, see e.g. [4, 5, 6]

Tungsten spectroscopy has several applications for a fusion plasma: it provides assessments of the tungsten influx to the plasma (and thus of the wall material sputtering rates and particle transport), the plasma power balance, and for diagnostics of plasma parameters. With tungsten distributed over the ITER plasma volume ions of various charge states allow for measurements of the local plasma conditions.

Several studies of tungsten spectra have been performed at tokamaks and other magnetically confined fusion plasmas, but the overwhelming majority of recent spectroscopic investigations of tungsten ions has been performed on electron beam ion traps (EBITs), notably the EBIT laboratories at Berlin (now decommisioned), NIST, Tokyo, and Livermore. Among these measurements are radiative and dielectronic recombination studies of L-shell W ions by Biedermann *et al.* [7], and Watanabe *et al.* [8]; M1 transitions in M-shell W ions by Ralchenko *et al.* [9]; optical transitions in highly charged W ions by Utter *et al.* [10], Komatsu *et al.* [11] and Watanabe *et al*. [12]; and intrashell x-ray transitions in L-shell W ions by Podpaly *et al.* [13]. At the Livermore EBIT facility the WOLFRAM project addresses the atomic data need on tungsten ions for fusion plasma diagnostics [14]. High-precision and spectral survey measurements are performed on the EBIT-I and SuperEBIT electron beam ion traps and complemented with measurements on fusion plasma experiments, such as the Livermore SSPX spheromak, the Princeton NSTX spherical torus, and the MIT Alcator C-Mod tokamak. Theoretical and modeling work are done in collaboration with groups at Livermore, the University of Nevada at Reno, and Lund University.

ATOMIC DATA FOR THE ITER CORE IMAGING X-RAY SPECTROMETER

The ion-temperature, T_i, and poloidal and toroidal rotation velocity, v_ϕ and v_θ, profiles of the ITER core plasmas will be measured using the Core Imaging X-ray Spectrometer (CIXS) [15]. The instrument is being designed for Doppler measurements of the L-shell spectra of highly charged tungsten ions. Centered on the spectrum of Ne-like W LXV, the $n = 2 – 3$ transitions fall in the 8 – 12 keV (1.0 – 1.5 Å) x-ray interval where the high-resolution crystal spectrometer will focus on one or a few spectral lines for measurements of line profiles and shifts. The CIXS may also include a broadband moderate-resolution x-ray calorimeter to facilitate diagnostics of the ITER core electron temperatures, T_e, and ion impurities [16]. To interpret the spectra and take full advantage of the diagnostic capabilities of the CIXS, accurate radiative and collisional data for W L- and M-shell ions are required [17]. Several spectroscopic studies on highly charged tungsten ions applicable to CIXS have been carried out using EBIT spectroscopy [7, 8, 18, 19, 20].

Tungsten has been chosen as the medium to probe the parameters of the ITER core plasmas since it will exist as an indigenous impurity element in ITER plasmas providing strong x-ray emission over a large electron-temperature interval. This is especially true for Ne-like W^{64+}, which, due to its closed-shell structure, has a fractional abundance of more than 10 % between 12 and 33 keV. Mid-Z elements predicted to be found in ITER plasmas, such as Ar (Z = 18), Fe (Z = 26), and Cu (Z = 29), will mostly be fully stripped in the core plasmas, with expected electron temperatures between 20 and 40 keV. An earlier design of the CIXS instrument was therefore open to the possibility of introducing Kr (Z = 36) into the tokamak for measurements of the He-like Kr XXXV spectrum [21]. To compare the strengths of the Kα emissions from He-like Kr XXXV to the L-shell transitions in Ne-like W LXV, the spectra have been calculated using the Flexible Atomic Code, FAC v.1.1.1 [22, 23] and modeled for steady-state ITER plasma conditions, see Table 1. The diagnostically interesting tungsten transitions have much higher emissivities than the krypton transitions[2]. However, it is important to note that the total ionization energy of almost 140 keV required to create a Ne-like W^{64+} ion [25] is about 3.5 times higher than the roughly 40 keV needed to make a He-like Kr^{34+} ion. Whereas tungsten is expected to be an intrinsic impurity in ITER plasmas, krypton would need to be injected. Even if tungsten would not exist in quantities sufficient to provide enough spectral signal, less tungsten than krypton will need to be introduced due to the much higher line emissivities. For a given signal strength, the energy consumed by W and Kr contribute about the same to the tokamak power balance (excluding bremsstrahlung).

This, of course, also strongly depends on the charge state distributions of tungsten and krypton ions and on the transport of the ions from the edge to the core plasmas[3].

In order to accurately infer the ion temperatures, T_i, and bulk rotational velocities, v_ϕ and v_ϕ, of the ITER plasmas from the Doppler effect, the rest line positions and shapes (strengths and widths) of the x-ray transitions must be well known from laboratory measurements. The very-high ion-temperatures in the core plasmas will broaden the lines to several electronvolts. Due to the high atomic mass of W, the Doppler widths of the x rays will be narrower for W than for Kr and mid-Z ions. Table 2 lists natural line widths together with Doppler widths of He-like Kr XXXV and Ne-like W LXV for temperatures of $T_e = T_i$ = 10, 20, 30, and 40 keV. Many of the listed transitions have very short upper level lifetimes, in particular Kr XXXV Kα w with 640 as and W LXV 3D with 350 as, giving rise to line broadenings of about 0.5 and 0.9 eV, respectively. For a typical CIXS spectrometer resolving power $R = E/\Delta E$ less than about 14000 it does not matter that Kr has narrower natural line widths than W. Conversely, for a spectrometer with a resolution close to, or below, the natural width of W 3D it is essential to know the exact line shape.

Spectral surveys and detailed measurements of W L-shell transitions have been performed at the Livermore EBIT facility [18, 19, 20]. Using a high-resolution crystal spectrometer in the von Hámos geometry at EBIT-I all the strong n = 2 – 3 lines in the Al-like W LXIII through O-like W LXVII spectra could be measured with high accuracy [20], see Fig. 1 for the Ne-like W LXV spectrum. Employing one of the x-ray calorimeter spectrometers from the Livermore–NASA laboratory astrophysics program [27], moderate-resolution spectra of W L-shell ions have been acquired at SuperEBIT for several electron excitation energies [19]. Shown in Fig. 1 is the 8 – 10 keV spectral region at E_{beam} = 23.5 keV where Ne-like W LXV dominates. Although the x-ray calorimeter may be operated to attain line widths below 5 eV at lower x-ray energies, the energy resolution achieved for this measurement was around 11 eV. The rapid development of x-ray calorimeters will likely result in energy resolutions of ~2 eV in the near future, making the addition of such an instrument to the CIXS diagnostic a practical option for broadband core impurity measurements [16].

The CIXS instrument design focuses on the Ne-like W LXV spectrum, in particular the 3D line, but, depending on the final spectrometer geometry and crystal selection, transitions from neighboring tungsten spectra may also be covered. This would then also allow for the core tungsten charge balance to be measured. Using FAC, collisional-radiative modeling of the W L-shell spectra have been performed to study how they develop with electron and ion

[2] It is furthermore easier to find crystals with appropriate 2d spacings and high reflectivities for W L-shell x rays than for Kr K-shell x rays.

temperatures. Figure 2 shows the calculated Ar-like W LVII through Li-like W LXXII spectra in the 8 – 10 keV interval for $T_e = T_i = 10$ and 30 keV.

ATOMIC DATA OF TUNGSTEN FOR EDGE AND OHMIC CORE PLASMAS

In plasmas of temperatures from a few hundred electronvolts to a few keV tungsten emission will be dominated by M- and N-shell transitions, mainly in the EUV and soft-x-ray parts of the spectrum. Since tungsten was first observed in tokamak plasmas in the mid-1970s by Isler *et al.* at the ORMAK tokamak [28] and by Hinnov *et al.* at the PLT tokamak [29], the strong quasicontinuum around 50 Å has been found in essentially all magnetically confined plasmas with tungsten impurity contents. Although this emission is extremely bright, the spectral complexity has prevented detailed diagnostic information to be extracted from it. The emission arises from $\Delta n = 0$ N-shell transitions from a multitude of N-shell tungsten charge states with transitions very close in energy. EBIT measurements at Berlin [30] and Livermore [31] have stepped through the tungsten charge states by varying the electron-beam energy and observing the resulting EUV emission. More detailed high-resolution measurements may discover useful diagnostic lines, something that could be very beneficial given the extremely strong emission over a wide electron-temperature range.

In keV-plasmas the W M-shell ions dominate the charge balance. The $n = 3 – 4$ spectra have been observed in ASDEX Upgrade plasmas [32], and EBIT experiments at NIST [33] and Livermore [34, 35, 36, 37] have measured many transitions in high resolution, especially in charge states near the closed-shell Ni-like W^{46+} ion. Figure 3 shows a measured spectrum from the Livermore EBIT-I at an electron-beam energy of 6.5 keV acquired with an x-ray calorimeter spectrometer with an energy resolution of 4.5 eV. The lines are identified by spectral modeling calculations and recognized as $n = 3 – 4$ transitions in Ge-like W^{42+} through Ti-like W^{52+} [14, 19].

Tungsten ions with 3s or 3p valence electrons have been studied in EBIT experiments at NIST [38, 39] and Livermore [40, 41]. The W ions isoelectronic to Na, W^{63+}, and Mg, W^{62+}, have $\Delta n = 0$ emission that should be strong also at core plasma temperatures. From these relatively simple spectra the complexity quickly develops going to lower charge states with more electrons, making the structure and spectra of most W ions with 3p and 3d valence electrons challenging to model accurately. Recently, $\Delta n = 0$ transitions in $W^{48+} – W^{61+}$ in the 27 – 40 Å interval were measured at the Livermore EBIT-I to provide benchmark data for electron-correlation calculations [41].

[3] The radiative cooling rates for a given charge balance of Kr have been studied at the Berlin EBIT facility [26].

ATOMIC DATA OF TUNGSTEN FOR ITER DIVERTOR DIAGNOSTICS

It will be important to monitor the concentration of tungsten ions in ITER divertor plasmas in order to infer the sputtering rates from the plasma-facing components. Furthermore, the large abundance of tungsten ions may also be applied for charge-balance, electron-temperature, and electron-density diagnostics. ITER divertor plasmas will be sufficiently cool (T_e around 1 eV close to the target plates and up to 150 eV near the X point) and dense ($N_e \sim 10^{15}$ cm^{-3}) so that only few-times charged tungsten ions will have large fractional abundances in thermodynamic equilibrium, cf. [42]. Only the spectra of the first few charge states have been studied [43, 44] and most of these investigations have been at electron densities much higher than magnetic fusion densities so that the spectra may not resemble the emission from tokamak divertors. Experiments to simulate this emission have been undertaken at the MT-1M tokamak [45], the Livermore SSPX spheromak [46], the Institute of Spectroscopy at the Russian Academy of Sciences and the Meudon Observatory [47], and, recently also at the Livermore EBIT facility.

The Sustained Spheromak Physics Experiment (SSPX) was the latest magnetic confinement experiment at Livermore, in operation from 1999 to 2007. The primary goals of the project was to investigate magnetic field build up and to evaluate the spheromak as a fusion reactor concept [48]. With modest electron temperatures (typically below 200 eV) and densities in the $10^{14–15}$ cm^{-3} range SSPX also provided a very suitable testbed for spectroscopic studies relevant to divertor plasmas of large tokamaks. Tungsten injection experiments provided enhancements to the intrinsic tungsten concentration (originating from the flux conserver coating) and aided the analysis of tungsten EUV spectra. Shown in Fig. 5 is a spectrum [46] acquired with a grazing-incidence instrument [49] at SSPX during injection of tungsten hexacarbonyl, $W(CO)_6$. As a result, both W and O line emission were enhanced. The strongest W emission is from Er-like W VII, which could be identified (though the line intensities do not agree) based on the sliding-spark measurements of Sugar and Kaufman [50]. The remaining emission attributed to tungsten is believed to belong to the neighboring charge states, but the complexity and modest spectral resolution have prevented definitive line identifications.

A more systematic study of the EUV spectra from few-times ionized tungsten have therefore been performed using EBIT spectroscopy. Operating the Livermore EBIT-I at low voltages, the excitation of tungsten spectra could be varied in the 30 – 300 eV range. Spectra in the 120 – 320 Å were acquired using a 5.6 m 1200 lines/mm grazing-incidence spectrometer (similar to the instrument used at SSPX) equipped with a Princeton Instruments CCD detector. High-resolution data of mainly Tm-like W VI, Er-like W VII, and Ho-like W VIII were obtained using a

44.3 m grating spectrometer [51]. Figure 5 illustrates the advantages of scanning the electron-beam energy for interpretation of plasma-produced spectra where the SSPX spectrum is followed by two panels with EBIT tungsten data at E_{beam} = 135 and 163 eV.

SUMMARY

Recent years' atomic spectroscopy efforts of tungsten ions have produced much atomic data important for power-balance estimates and diagnostics of magnetically confined plasmas. Still, since tungsten impurity ions in future plasma devices can be expected to be found both in cooler regions, such as divertor and near-wall plasmas, as well as in moderate and hot regions, such as edge and core plasmas, there is a significant need for additional radiative and collisional data on tungsten in essentially all ionization stages. Presented in this paper is an overview of recent results from the Livermore WOLFRAM project, which has produced data on L- and M-shell W ions important for the ITER CIXS instrument, M-shell W ions for ITER edge and present-day plasmas, and O-shell W ions for ITER divertor diagnostics.

ACKNOWLEDGMENTS

Work was performed at Lawrence Livermore National Laboratory under the auspices of the U.S. Department of Energy under contract DE-AC52-07NA27344 and carried out as part of the International Atomic Energy Agency Coordinated Research Project *Spectroscopic and Collisional Data for Tungsten from 1 eV to 20 keV*. The authors wish to acknowledge support from Dr. M. F. Gu and Mr. E. W. Magee.

REFERENCES

1. R. A. Pitts, A. Kukushkin, A. Loarte, A. Martin, M. Merola, C. E. Kessel, V. Komarov, and M. Shimada, *Phys. Scr.* **T138**, 014001 (2009)
2. G. F. Matthews, M. Beurskens, S. Brezinsek, M. Groth, E. Joffrin, A. Loving, M. Kear, M.-L. Mayoral, R. Neu, P. Prior, V. Riccardo, F. Rimini, M. Rubel, G. Sips, E. Villedieu, P. de Vries, M. L. Watkins, and EFDA-JET contributors, *Phys. Scr.* **T145**, 014001 (2011)

3. R. Neu, V. Bobkov, R. Dux, J. C. Fuchs, O. Gruber, A. Herrmann, A. Kallenbach, H. Maier, M. Mayer, T. Pütterich, V. Rohde, A. C. C. Sips, J. Stober, K. Sugiyama, and ASDE Upgrade Team, *Phys. Scr.* **T138**, 014038 (2009)
4. M. B. Chowdhuri, S. Morita, M. Goto, H. Nishimura, K. Nagai, and S. Fujioka, *Plasma Fusion Res.* **2**, S1060 (2007)
5. C. S. Harte, C. Suzuki, T. Kato, H. A. Sakaue, D. Kato, K. Sato, N. Tamura, S. Sudo, R. D'Arcy, E. Sokell, J. White, and G. O'Sullivan, *J. Phys. B: At. Mol. Opt. Phys.* **43**, 205004 (2010)
6. J. Clementson, P. Beiersdorfer, A. L. Roquemore, C. H. Skinner, D. K. Mansfield, K. Hartzfeld, and J. K. Lepson, *Rev. Sci. Instrum.* **81**, 10E326 (2010)
7. C. Biedermann, R. Radtke, R. Seidel, and T. Pütterich, *Phys. Scr.* **T134**, 014026 (2009)
8. H. Watanabe, N. Nakamura, D. Kato, T. Nakano, and S. Ohtani, *Plasma Fusion Res.* **2**, 027 (2007)
9. Yu. Ralchenko, I. Draganić, D. Osin, J. D. Gillaspy, and J. Reader, *Phys. Rev. A* **83**, 032517 (2011)
10. S. B. Utter, P. Beiersdorfer, and G. V. Brown, *Phys. Rev. A* **61**, 030503(R) (2000)
11. A. Komatsu, J. Sakoda, N. Nakamura, H. A. Sakaue, X.-B. Ding, D. Kato, I. Murakami, and F. Koike, *Phys. Scr.* **T144**, 014012 (2011)
12. H. Watanabe, N. Nakamura, D. Kato, H. A. Sakaue, S. Ohtani, Can. J. Phys. 90, 497 (2012)
13. Y. Podpaly, J. Clementson, P. Beiersdorfer, J. Williamson, G. V. Brown, and M. F. Gu, *Phys. Rev. A* **80**, 052504 (2009)
14. J. Clementson, P. Beiersdorfer, G. V. Brown, M. F. Gu, H. Lundberg, Y. Podpaly, and E. Träbert, *Can. J. Phys.* **89**, 571 (2011)
15. P. Beiersdorfer, J. Clementson, J. Dunn, M. F. Gu, K. Morris, Y. Podpaly, E. Wang, M. Bitter, R. Feder, K. W. Hill, D. Johnson, and R. Barnsley, *J. Phys. B: At. Mol. Opt. Phys.* **43**, 144008 (2010)
16. P. Beiersdorfer, G. V. Brown, J. Clementson, J. Dunn, K. Morris, E. Wang, R. L. Kelley, C. A. Kilbourne, F. S. Porter, M. Bitter, R. Feder, K. W. Hill, D. Johnson, and R. Barnsley, *Rev. Sci. Instrum.* **81**, 10E323 (2010)
17. J. Clementson, P. Beiersdorfer, C. Biedermann, M. Bitter, L. F. Delgado-Aparicio, A. Graf, M. F. Gu, K. W. Hill, and R. Barnsley, *Europhys. Conf. Abs.* **36**, P2.040 (2012)
18. P. Beiersdorfer, *AIP Conf. Proc.* **274**, 365 (1993)
19. J. Clementson, *Ph.D. Dissertation*, Lund University (2010)

20. P. Beiersdorfer, J. K. Lepson, M. B. Schneider, and M. P. Bode, *Phys. Rev. A* **86**, 012509 (2012)

21. R. Barnsley, M. O'Mullane, L. C. Ingesson, and A. Malaquias, *Rev. Sci. Instrum.* **75**, 3743 (2004)

22. M. F. Gu, *AIP Conf. Proc.* **730**, 127 (2004)

23. M. F. Gu, *Can. J. Phys.* **86** 675 (2008)

24. K. Widmann, P. Beiersdorfer, V. Decaux, and M. Bitter, *Phys. Rev. A* **53**, 2200 (1996)

25. P. Beiersdorfer, M. J. May, J. H. Scofield, and S. B. Hansen, *High Energy Density Phys.* **8**, 271 (2012)

26. R. Radtke, C. Biedermann, T. Fuchs, G. Fußmann, and P. Beiersdorfer, *Phys. Rev. E* **61**, 1966 (2000)

27. F. S. Porter, J. S. Adams, P. Beiersdorfer, G. V. Brown, J. Clementson, M. Frankel, S. M. Kahn, R. L. Kelley, and C. A. Kilbourne, *AIP Conf. Proc.* **1185**, 454 (2009)

28. R. C. Isler, R. V. Neidigh, and R. D. Cowan, *Phys. Lett.* **63 A**, 295 (1977)

29. E. Hinnov and M. Mattioli, *Phys. Lett.* **66 A**, 109 (1978)

30. R. Radtke, C. Biedermann, J. L. Schwob, P. Mandelbaum, and R. Doron, *Phys. Rev. A* **64**, 012720 (2001)

31. S. B. Utter, P. Beiersdorfer, and E. Träbert, *Can. J. Phys.* **80**, 1503 (2002)

32. R. Neu, K. B. Fournier, D. Schlögl, and J. Rice, *J. Phys. B: At. Mol. Opt. Phys.* **30**, 5057 (1997)

33. Yu. Ralchenko, J. N. Tan, J. D. Gillaspy, J. M. Pomeroy, and E. Silver, *Phys. Rev. A* **74**, 042514 (2006)

34. P. Neill, C. Harris, A. S. Safronova, S. Hamasha, S. Hansen, U. I. Safronova, and P. Beiersdorfer, *Can. J. Phys.* **82**, 931 (2004)

35. J. Clementson, P. Beiersdorfer, G. V. Brown, and M. F. Gu, *Phys. Scr.* **81**, 015301 (2010)

36. J. Clementson, P. Beiersdorfer, and M. F. Gu, *Phys. Rev. A* **81**, 012505 (2010)

37. C. G. Osborne, A. S. Safronova, V. L. Kantsyrev, U. I. Safronova, P. Beiersdorfer, K. M. Williamson, M. E. Weller, and I. Shresta, *Can. J. Phys.* **89**, 599 (2011)

38. Yu. Ralchenko, I. N. Draganic, J. N. Tan, J. D. Gillaspy, J. M. Pomeroy, J. Reader, U. Feldman, and G. E. Holland, *J. Phys. B: At. Mol. Opt. Phys.* **41**, 021003 (2008)

39. J. D. Gillaspy, I. N. Draganić, Yu. Ralchenko, J. Reader, J. N. Tan, J. M. Pomeroy, and S. M. Brewer, *Phys. Rev. A* **80**, 010501(R) (2009)

40. J. Clementson and P. Beiersdorfer, *Phys. Rev. A* **81**, 052509 (2010)

41. T. Lennartsson, J. Clementson, and P. Beiersdorfer, *Phys. Rev. A*, in preparation (2012)

42. A. E. Kramida and J. Reader, *At. Data Nucl. Data Tables* **92**, 457 (2006)

1 43. A. E. Kramida and T. Shirai, *At. Data Nucl. Data Tables* **95**, 305 (2009)

2 44. A. Kramida, *Can. J. Phys.* **89**, 551 (2011)

3 45. G. Veres, J. S. Bakos, and B. Kardon, *J. Quant. Spectrosc. Radiat. Transfer* **56**, 295 (1996)

4 46. J. Clementson, P. Beiersdorfer, E. W. Magee, H. S. McLean, R. D. Wood, *J. Phys. B: At. Mol. Opt. Phys.* **43**,
5 144009 (2010)

6 47. W.-Ü. L. Tchang-Brillet, J.-F. Wyart, A. N. Ryabtsev, R. R. Kildiyarova, and E. Ya. Kononov, *ASOS 10 Book of*
7 *Abstracts*, Berkeley, California (2010)

8 48. B. Hudson, R. D. Wood, H. S. McLean, E. B. Hooper, D. N. Hill, J. Jayakumar, J. Moller, D. Montez, C. A.
9 Romero-Talamás, T. A. Casper, J. A. Johnson III, L. L. DoDestro, E. Mezonlin, and L. D. Pearlstein, Phys.
10 Plasmas 15, 056112 (2008)

11 49. J. Clementson, P. Beiersdorfer, and E. W. Magee, *Rev. Sci. Instrum.* **79**, 10F538 (2008)

12 50. J. Sugar and V. Kaufman, *Phys. Rev. A* **12**, 994 (1975)

13 51. P. Beiersdorfer, E. W. Magee, E. Träbert, H. Chen, J. K. Lepson, M.-F. Gu, and M. Schmidt, Rev. Sci. Instrum.
14 75, 3723 (2004)

TABLE 1. Predicted transition emissivities for electron-impact excitation in He-like Kr XXXV and Ne-like W LXV for plasmas with $N_e = 10^{14}$ cm^{-3} and T_e = 10, 20, 30, and 40 keV. Emissivities ε are listed in units of photon per ion per second (γ/Z^{q+}/s). Experimental transition energies ΔE_{exp}, are in units of electronvolt (eV).

Line	ΔE_{exp}	**ε (10 keV)**	**ε (20 keV)**	**ε (30 keV)**	**ε (40 keV)**
Kr XXXV Kα w ($1s_{1/2} - 2p_{3/2}$)	13114.68(36)[a]	45	82	101	111
Kr XXXV Kα x ($1s_{1/2} - 2p_{3/2}$)	13091.17(37)[a]	7	7	6	5
Kr XXXV Kα y ($1s_{1/2} - 2p_{1/2}$)	13026.29(36)[a]	16	26	30	32
Kr XXXV Kα z ($1s_{1/2} - 2s_{1/2}$)	12979.63(41)[a]	8	9	9	8
W LXV 3A ($2s_{1/2} - 3p_{3/2}$)	10706.85(90)[b]	24	42	49	54
W LXV 3C ($2p_{1/2} - 3d_{3/2}$)	10408.69(40)[b]	146	217	244	257
W LXV 3B ($2s_{1/2} - 3p_{1/2}$)	10317.23(50)[b]	48	76	87	93
W LXV 3F ($2p_{1/2} - 3d_{3/2}$)	9689.29(50)[b]	46	57	57	55
W LXV 3D ($2p_{3/2} - 3d_{5/2}$)	9126.25(50)[b]	497	695	766	798
W LXV 3E ($2p_{3/2} - 3d_{3/2}$)	8996.31(50)[b]	27	32	33	32
W LXV 3G ($2p_{3/2} - 3s_{1/2}$)	8307.51(40)[b]	288	358	367	356
W LXV M2 ($2p_{3/2} - 3s_{1/2}$)	8299.22(40)[b]	106	132	115	96

[a]Widmann *et al.* [24], [b]Beiersdorfer *et al.* [20]

TABLE 2. Calculated line widths for He-like Kr XXXV and Ne-like W LXV. ΔE_N refers to natural broadening and ΔE_D to Doppler broadening for T_i = 10, 20, 30, and 40 keV. Units in electronvolt (eV).

Line	ΔE_N	ΔE_D **(10 keV)**	ΔE_D **(20 keV)**	ΔE_D **(30 keV)**	ΔE_D **(40 keV)**
Kr XXXV Kα w ($1s_{1/2} - 2p_{3/2}$)	0.52	7.44	10.53	12.89	14.89
Kr XXXV Kα x ($1s_{1/2} - 2p_{3/2}$)	0.00	7.43	10.51	12.87	14.86
Kr XXXV Kα y ($1s_{1/2} - 2p_{1/2}$)	0.13	7.39	10.46	12.81	14.79
Kr XXXV Kα z ($1s_{1/2} - 2s_{1/2}$)	0.00	7.37	10.42	12.76	14.73
W LXV 3A ($2s_{1/2} - 3p_{3/2}$)	0.16	6.08	8.59	10.53	12.15
W LXV 3C ($2p_{1/2} - 3d_{3/2}$)	0.49	5.91	8.35	10.23	11.81
W LXV 3B ($2s_{1/2} - 3p_{1/2}$)	0.23	5.86	8.28	10.14	11.71
W LXV 3F ($2p_{1/2} - 3d_{3/2}$)	0.01	5.50	7.77	9.52	10.99
W LXV 3D ($2p_{3/2} - 3d_{5/2}$)	0.95	5.18	7.32	8.97	10.35
W LXV 3E ($2p_{3/2} - 3d_{3/2}$)	0.03	5.10	7.22	8.84	10.21
W LXV 3G ($2p_{3/2} - 3s_{1/2}$)	0.05	4.71	6.66	8.16	9.43
W LXV M2 ($2p_{3/2} - 3s_{1/2}$)	0.00	4.71	6.66	8.15	9.42

1

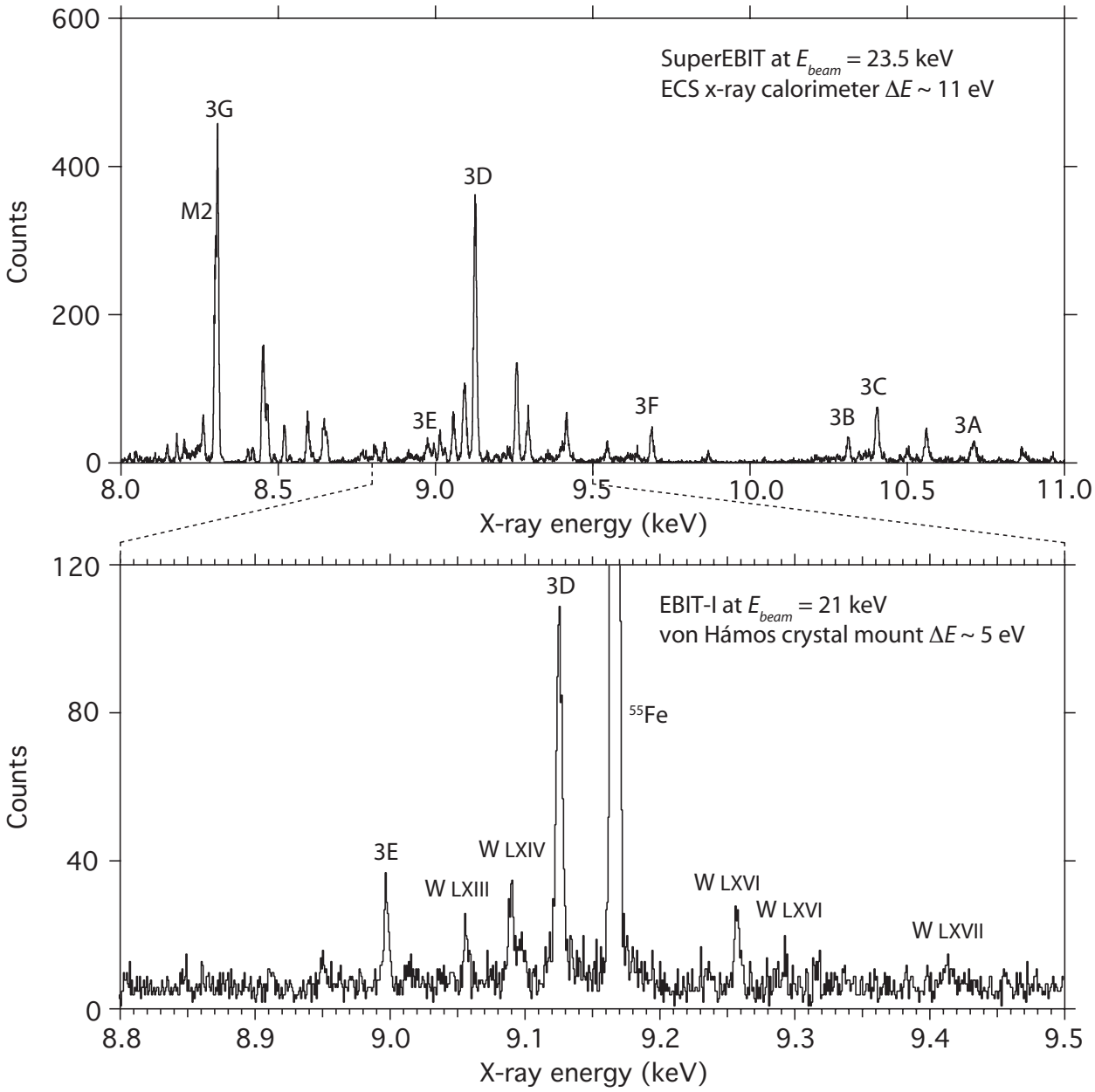

FIGURE 1. Ne-like W LXV spectra measured at the Livermore EBIT facility using a NASA x-ray calorimeter spectrometer [19] and a von Hámos crystal spectrometer [20].

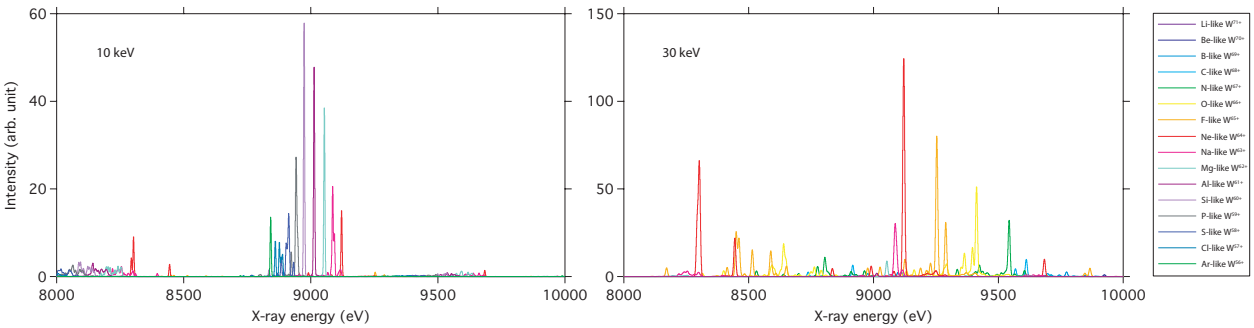

FIGURE 3. Theoretical spectra of W LVII – LXXII for $T_e = T_i = 10$ and 30 keV and $N_e = 10^{14}$ cm^{-3}.

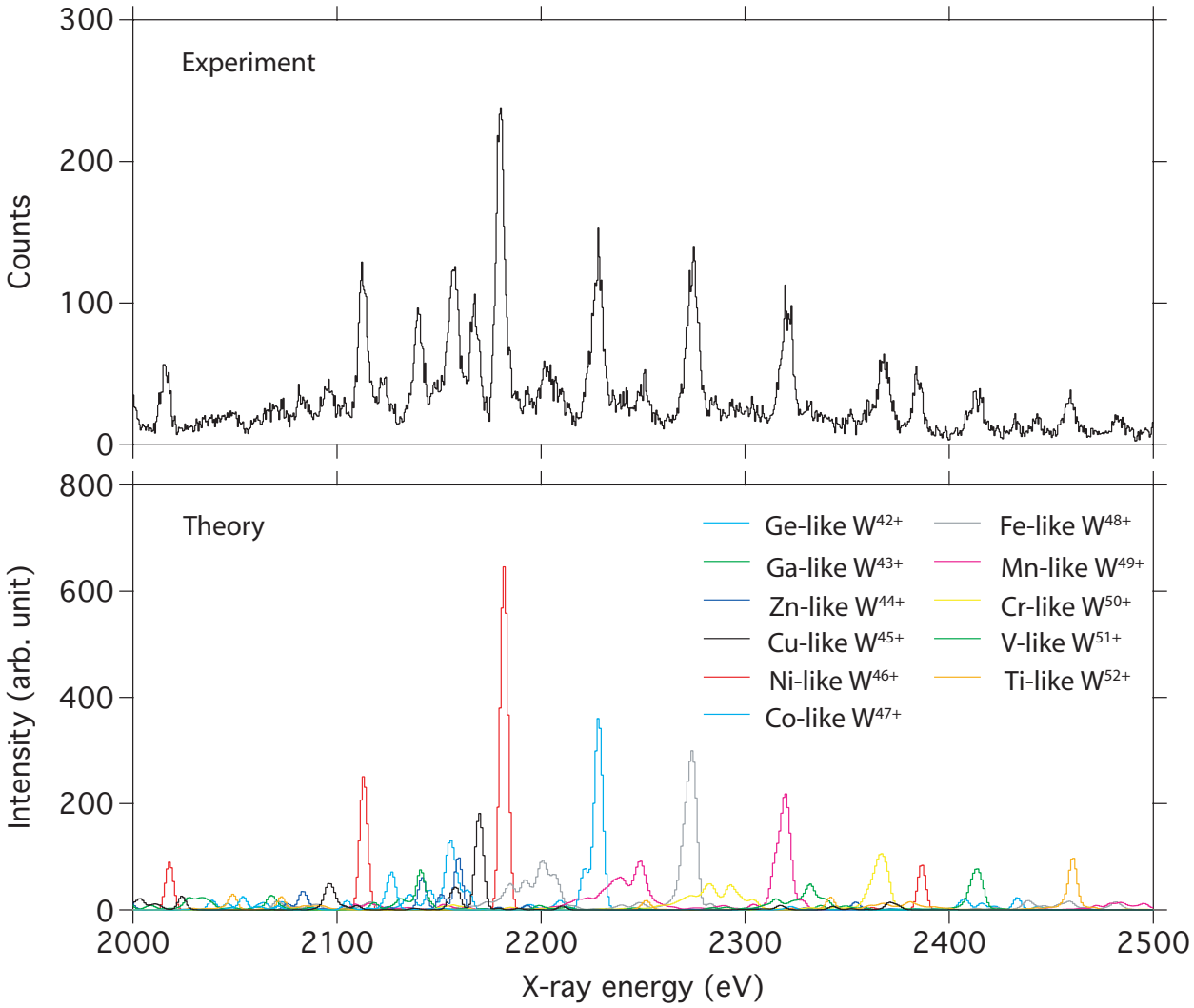

FIGURE 4. M-shell transitions from M- and N-shell charge states of tungsten measured at the Livermore EBIT-I for $E_{beam} = 6.5$ keV and compared to collisional-radiative modeling [14, 19].

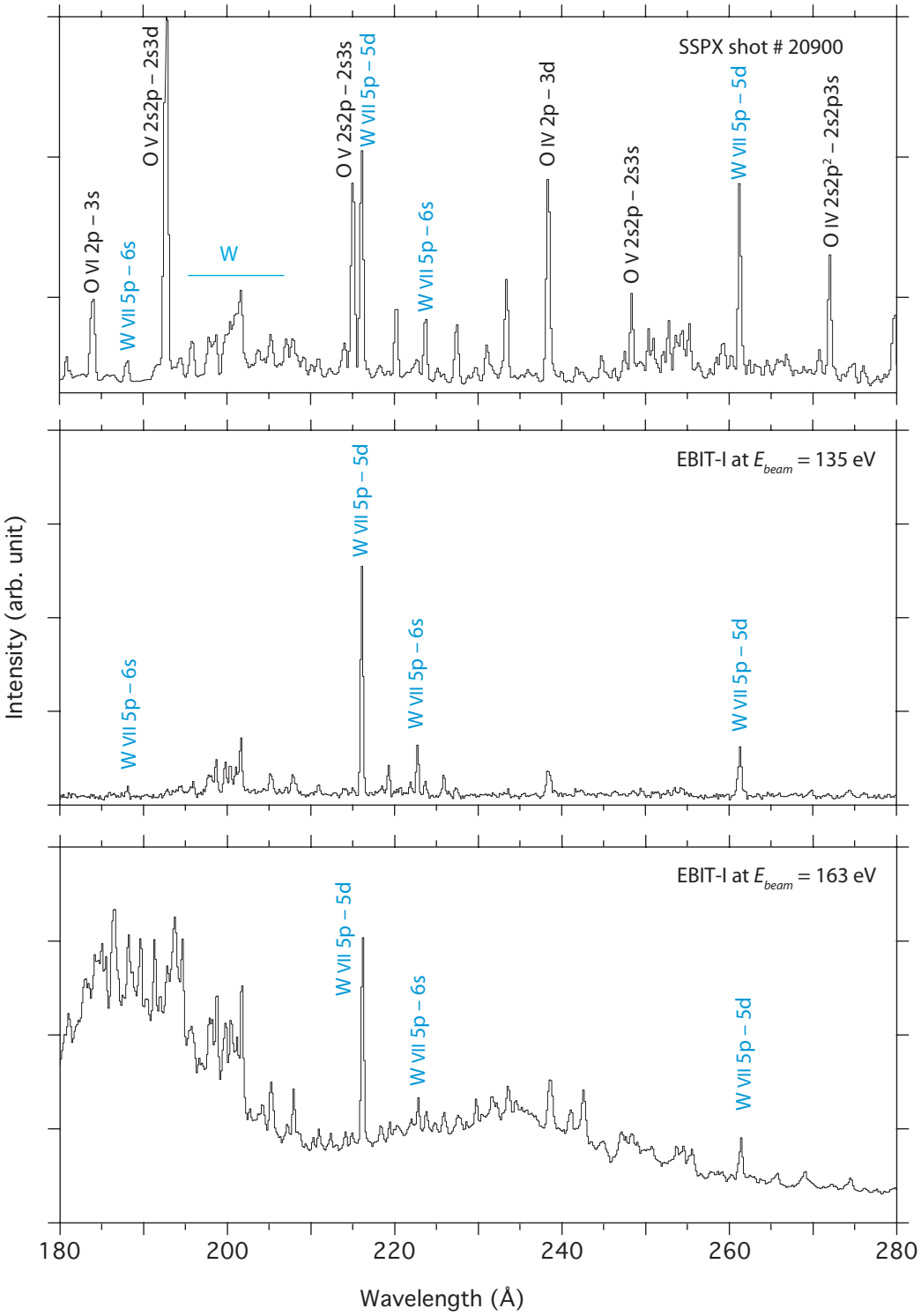

FIGURE 5. Spectra from low charge states of tungsten measured at the Livermore SSPX spheromak and the Livermore EBIT-I electron beam ion trap. Lines not labeled in the SSPX spectrum are mainly from W, O, and Ti.